

# RADICAL-Pilot and Parsl: Executing Heterogeneous Workflows on HPC Platforms

Aymen Alsaadi<sup>1</sup>, Andre Merzky<sup>1</sup>, Kyle Chard<sup>3,4</sup>, Shantenu Jha<sup>1,2</sup>, Matteo Turilli<sup>1,2</sup>

<sup>1</sup> Rutgers, the State University of New Jersey, Piscataway, NJ 08854, USA

<sup>2</sup> Brookhaven National Laboratory, Upton, NY 11973, USA

<sup>3</sup> Department of Computer Science, University of Chicago, Chicago, IL, USA

<sup>4</sup> Data Science and Learning Division, Argonne National Laboratory, Argonne, IL, USA

**Abstract**—Executing scientific workflows with heterogeneous tasks on HPC platforms poses several challenges which will be further exacerbated by the upcoming exascale platforms. At that scale, bespoke solutions will not enable effective and efficient workflow executions. In preparation, we need to look at ways to manage engineering effort and capability duplication across software systems by integrating independently developed, production-grade software solutions. In this paper, we integrate RADICAL-Pilot (RP) and Parsl and develop an MPI executor to enable the execution of workflows with heterogeneous (non)MPI Python functions at scale. We characterize the strong and weak scaling of the integrated RP-Parsl system when executing two use cases from polar science, and of the function executor on both SDSC Comet and TACC Frontera. We gain engineering insight about how to analyze and integrate workflow and runtime systems, minimizing changes in their code bases and overall development effort. Our experiments show that the overheads of the integrated system are invariant of resource and workflow scale, and measure the impact of diverse MPI overheads. Together, those results define a blueprint towards an ecosystem populated by specialized, efficient, effective and independently-maintained software systems to face the upcoming scaling challenges.

**Index Terms**—Workflows, HPC, Heterogeneity.

## I. INTRODUCTION

Exascale computing and the forthcoming generation of high-performance computing (HPC) platforms will enable execution of scientific workflows at unprecedented scale but doing so will present many new challenges. Perhaps the most significant is the need for the middleware that enables the execution of scientific workflows to use the available resources effectively and efficiently, while providing the large array of capabilities required by diverse use cases and domain scientists. At exascale, this challenge will make it infeasible to apply ad hoc approaches to workflow development, as bespoke solutions, glue software written to enable a specific use case, and software systems prototyped by students and postdocs, are unable to satisfy the requirements of workflows execution.

Scientific workflows and HPC are converging at unprecedented pace and task heterogeneity is at the core of modern scientific workflows. Tasks may take many forms, from standalone executables, developed by scientific communi-

ties with decades of established adoption, or functions implemented in diverse programming languages and tailored to specific use cases. Both executable and function tasks have diverse requirements: from large MPI simulation executables, to MPI analysis functions or single-core utility functions. Task heterogeneity requires specific capabilities across the middleware stack to enable users to express diverse types of tasks while having a runtime system capable of interpreting and managing the execution of those tasks at scale and on diverse HPC platforms.

Matching the challenges posed by executing heterogeneous workflows on HPC resources at ever increasing scale requires a suitable ecosystem of middleware components. That ecosystem has to build upon existing solutions that are robust, properly packaged, distributed and maintained, and have proven adoption among relevant scientific communities. Further, those tools need to implement new capabilities when necessary or be integrated where possible, minimizing code and effort duplication across the stack. In contrast to other ‘framework’ approaches, this ecosystem would not be a single, end-to-end software stack maintained by a specific group but, instead, a coordinated set of tools developed and maintained by independent groups. Those groups would follow policies and best practices agreed upon, not dissimilar to what is routinely done by the open source community.

In this paper, we present a first step towards realizing that ecosystem. We integrated two existing, independently developed software systems and executed the workflows of two exemplar use cases on HPC resources. Based on our previous experience with integrating independent systems [1], [2], [11] and our building blocks approach [3], we describe an integration that minimizes changes in the existing code-bases while allowing users to benefit from the capabilities of both systems. We show how to approach the integration, evaluate diverse integration points and align the programming and execution models of the two systems. While we are still far from exascale and its ultimate use cases, the integration we present works as a blueprint of our approach, indicating how to progress forward.

We integrate RADICAL-Pilot (RP) [4], [5], a pilot system that enables the execution of multi-task, heterogeneous workloads on diverse HPC platforms, and Parsl [6],

a parallel scripting library for Python that provides workflow and dataflow capabilities. The result is a loosely-coupled system that does not require a dedicated code repository but only an interface with a small code footprint. Via the RP-Parsl integration, users can describe workflow application in Parsl and use RP capabilities to acquire HPC resources and manage the execution of the workflow’s tasks on them. Users benefit from the capabilities of the two systems but no capability duplication is required between RP and Parsl.

Once integrated, we show how RP-Parsl supports the execution of two heterogeneous workflows and workloads from two polar science use cases on HPC resources. Supporting those workflows is challenging because they require execution of heterogeneous tasks coded as Python functions, some of which use the message passing interface (MPI). We developed an executor for RP to support the concurrent execution of MPI Python functions at scale on HPC resources. The RP-Parsl integration makes the MPI capabilities of that RP executor immediately available via Parsl, without the need for further engineering.

We characterize the strong and weak scaling of both the executor and the use cases’ workflows, analyzing the overheads of the proposed integration and executor. The experiments break down the performance of the executor, `mpirun`, and `mpi4py` on both SDSC Comet and TACC Frontera HPC platforms. We show that RP-Parsl supports the workflows of the two use cases with overheads which are invariant of scale and relatively small compared to the total execution time. The insight gained by our analysis shows the viability of the proposed integrative approach and offers useful information about how to further improve the concurrent execution of Python MPI functions at scale on HPC resources.

## II. RELATED WORK

The integration of workflow and runtime systems extends functionalities and interfaces, enabling different programming paradigms and the execution of different applications, on different platforms and at a larger scale.

Kepler [7] and Hadoop [8] integration [9] enables high scalability, fault tolerance, and the usage of MapReduce in Kepler scientific workflows on HPC platforms. That integration allows users to create Hadoop jobs with ease via a GUI but it also requires users to setup and configure a distributed Hadoop cluster on the HPC platform. Hadoop-on-HPC [2] integrates Hadoop with RADICAL-Pilot (RP): Hadoop extends RP with the MapReduce programming paradigm, and RP’s pilot capabilities enable deployment of the Hadoop cluster and scheduling of the workflow’s tasks on that cluster.

Different from Hadoop-Kepler and Hadoop-on-HPC, the integration between Swift [10] and RP show the benefits of integrating systems based on their application programming interfaces (API) and special-purpose connectors. That approach reduces the engineering effort spent

on each system, centering the development on a small and independent component that translates computational requirements between the workflow application layer, and the resource management and task execution layers. Note that Swift requires users to adopt a domain-specific language to code their application workflows, increasing the learning curve and limiting reusability across applications.

The integration between Parsl and WorkQueue [11] shows the possibility of achieving better performance and resource utilization by using dynamic resource management and the WorkQueue framework [12]. The integration uses Parsl API, which does not support resource specifications at task level. WorkQueue and Parsl use a technique for lightweight function monitoring across the resources, which forks a new process for every function, introducing additional resource requirements that might not be possible on HPC and local platforms.

Merlin [13] is designed to enable the execution of large ensembles simulations and machine learning analyses on HPC platforms. Merlin uses Maestro [14] as an interface to define robust and complex workflows of millions of tasks. Further, Merlin deploys Flux [15] to interact with HPC to scale to a large number of jobs. Merlin uses Maestro YAML-based interface to define tasks in a shell syntax only, making it challenging for the end-user to take advantage of clearer and more powerful programming language, such as Python.

The integration [16] of StarPU [17] and the SkePU [18] is a good example of integrating a high-level parallel programming paradigm to define computational patterns that can be executed with StarPU tasks. The integration brings many of StarPU’s capabilities to SkePU, such as data partitioning and various scheduling strategies. In turn, StarPU acquires a high-level interface that supports the execution of data-parallel computations. The integration requires C++ and offers a limited number of skeletons.

In this paper, we build upon the lessons learned by integrating RP with Hadoop and Swift, and the insight from the integrations between parallel programming environments and runtime systems to integrate Parsl and RP. We reduce the engineering required by the integration, developing a lightweight API-level connector for Parsl and RP, and we develop an executor for RP to enable MPI function-level parallelism for functions written in Python and parallelized via Parsl. In that way, we enable writing workflow applications with MPI Python functions and execute them on diverse HPC platforms at scale.

## III. USE CASES

We present two exemplar use cases that require the capabilities of both RP and Parsl to execute MPI and non-MPI Python functions on HPC platforms. We focus on the specification, computational and functional requirements of every use case.

### A. Satellite Imagery Geolocation

High-resolution satellite and aerial imagery analysis are crucial for practical monitoring of ice sheet volume change, mass, and sea-level rise. As the datasets increase in volume and number of images, utilizing HPC resources to process those images becomes necessary. Scaling the image processing on HPC platforms is challenging, mostly because of the available amount of computational resources and human labor it needs. The solution is developing workflows to automate the processing of images at scale.

Image geolocation appends geographical metadata to images. Each image is paired to other images, and relevant image features are algorithmically extracted, compared and matched. On the base of those features, datasets of geographical areas recorded at different points in time, by different tools, with different camera viewpoints, orientation, resolution, and brightness can be matched.

The geolocation workflow has two types of tasks: image matching, using the scale-invariant feature transform (SIFT) algorithm [19], and image rectifying, using the random sampling consensus (RANSAC) algorithm [20]. Image matching uses the CUDA-C++ GPU-SIFT [21] executable to match similar features in an image pair. Image rectifying uses the OpenCV RANSAC [22] Python function to eliminate false-positive outliers from the SIFT application’s output and produce better matches [23].

### B. Ice Wedge Polygons

Ice wedges are common permafrost subsurface attributes that evolved by accumulated frost cracking and ice-vein growth over long periods of time. These wedge-shaped ice masses create polygonized land surface patterns called Ice Wedge Polygons (IWP) across large Arctic areas. Observing IWP requires processing very high spatial resolution (VHSR) satellite imageries at multiple spatial scales [24].

IWP is implemented via MPI Python functions that require both GPUs and CPUs concurrently. Each image is processed by performing two operations—tiling and inference—both implemented as MPI Python functions. Tiling uses CPUs to divide each image into hundreds of  $360 \times 360$  pixels tiles. Once the tiling is done, the inference operation uses a GPU to extract the surface patterns from a tile, saving them into a ‘shape file’. All the shape files of an image’s tiles are then stitched together and converted into a human interpretable image.

## IV. RADICAL-PILOT AND PARSL INTEGRATION

We integrate RP and Parsl into a system named, for simplicity, RP-Parsl. Note that we do not create a new, independent system but, instead, an interface between the two systems ‘as they are’. That provides users with the sum of the two systems’ capabilities without the need to reengineer a whole new system.

### A. RADICAL-Pilot (RP)

RP is a scalable, modular, and interoperable pilot system coded in Python. RP enables the execution of diverse and dynamic workloads on heterogeneous HPC resources. RP supports the concurrent execution of heterogeneous tasks by using multilevel scheduling of jobs and tasks. Fig. 1 shows the four main components of RP’s architecture (purple boxes): The Pilot-Manager and the Task-Manager, which are executed on users’ resources or on the login node of the HPC platform; the Agent, which is executed on the compute nodes of the target HPC platform; and a MongoDB database, which is hosted on resources accessible via network by the other components.

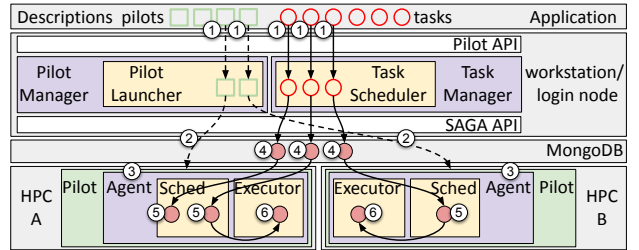


Fig. 1. RADICAL-Pilot architecture and execution model.

Traditionally, executing many tasks on HPC platforms presents several challenges, including efficiently and effectively scheduling, placing and launching independent tasks across multiple compute nodes. RP uses the pilot abstraction [25] to support the concurrent execution of up to  $10^6$  tasks on  $10^3$  compute nodes with affordable overheads [5]. Different from other pilot systems, RP supports four types of tasks: (1) single/multi cores/GPUs with MPI, OpenMP, single/multi threaded and single/multi process tasks; (2) tasks requiring between 1 and 27,000 GPUs and/or 1 and 467,000 CPU cores; (3) tasks with duration from  $>1$  second to 24 hours; and (4) tasks implemented either as standalone executables or Python functions.

### B. Parsl

Parsl is a parallel scripting library for Python that relies on function decorators to express parallelism [6], while exposing a lightweight and straightforward API. Users can annotate a well-defined Python function (input, output, and commands) with a Parsl decorator to indicate that the function can be executed in parallel. Parsl’s runtime system then enacts that parallelism, abstracting away from the users the complexities of its management.

Fig. 2 shows the three main components of Parsl: Data Flow Kernel (DFK), Executor, and Provider. The life cycle of a Parsl application starts by calling annotated functions (Parsl ‘apps’) and passing one or more task descriptions to the DFK that, in turn, represents tasks’ data dependencies as a directed acyclic graph (DAG). The DFK wraps that task with a Python future object [26] and, once a task’s dependencies are resolved, the DFK submits it to one of

the user-specified executors. The DFK tracks every task’s state and updates the task graph accordingly.

Parsl relies on Python’s standard `concurrent.futures` executor interface. It includes three in-built executors that confirm to this interface, each designed to execute a type of workload. The high-throughput executor (HTEX) is a pilot-based executor for high-throughput execution of short and long-running tasks. The Extreme-Scale Executor (EXEX) executes tasks on a pool of multi-node processes. The EXEX executor is based on the Python package `mpi4py` [27] to build and manage the communications between the managers and the workers. The Low Latency Executor (LLEX) is built to execute fast tasks that require near-real-time execution.

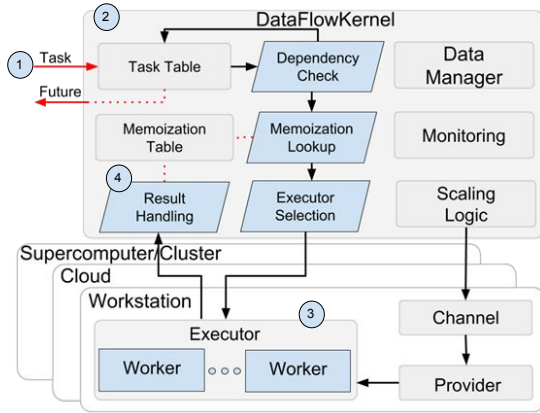


Fig. 2. Parsl architecture and execution model.

### C. Design

Based on Figs. 1 and 2, RP and Parsl present at least two integration points: using RP to submit one of Parsl’s existing executors or using RP Agent as a new executor for Parsl. While the former would allow Parsl’s users to reduce the effort currently required to acquire and provision HPC resources, it would not allow users to benefit from most of RP’s Agent capabilities. The second integration option allows us to instead maintain all Parsl API and workflow-related capabilities alongside all RP’s runtime capabilities.

Compared to Parsl, RP is focused on providing MPI support across multiple HPC platforms and supporting multiple dimension of tasks and resource heterogeneity. Further, RP supports Single Program Multiple Data (SPMD) and its performance is tailored to extreme-scale on HPC resources [5]. Other differences include concurrently executing multiple pilots on multiple HPC platforms [28] and scheduling a single workload across those pilots [1]. While RP and Parsl’s runtime systems already share a set of runtime capabilities, their integration will avoid future duplications and promote specialization in different areas of the end-to-end process of executing workflows on the upcoming exascale HPC platforms.

Integrating RP as a Parsl executor requires aligning the two systems’ task execution models. RP implements an

agent-based parallel processing model with one or more Agents, each launched by the Pilot Manager on a compute node of the target HPC platform. (1.1–3). RP Task Manager schedules tasks on an Agent (1.4) and the Agent’s Scheduler schedules those tasks on the Executor (1.5) that launches them on the acquired HPC resources (1.6).

RP’s tasks are fully-decoupled, i.e., they have no data dependencies or those dependencies have been already satisfied out-of-band. Each task is assumed to be self-contained, executed by RP as a black-box that either returns or fails. RP has no control or knowledge about the code each task executes, enabling a clean separation of concern between resource management, execution management and task executables. Consistently, at application level, RP implements a ‘batch-like’ programming model in which groups of tasks (i.e., workloads) are described and then submitted for execution. Concurrency is implicit as users do not have to control it: once submitted, RP executes tasks with the maximum concurrency allowed by the available resources.

Parsl’s HTEX executor implements a manager-worker parallel processing model in which each manager occupies a compute node on a HPC, cluster or cloud platform, and controls several workers. Parsl DFK creates a task table and adds the tasks to it once it’s received (2.1–2). The DFK prepares the task for execution (2.3–4) and sends them to the executor (2.4). Then, the executor’s manager assigns every task to a specific worker (2.5) and returns the results to the DFK (2.6).

Unlike RP tasks, Parsl tasks are coupled, and they have dynamic data dependencies that must be respected before reaching the executor level. At the application level, Parsl allows for the expression of nested parallelism within a single task or across a batch of tasks. Parsl programming model enables various parallel computing paradigms such as procedural and dynamic workflow execution and interactive parallel programming.

Parsl’s tasks are Python functions while RP tasks are Python dictionaries whose content is dynamically updated to reflect the state of the tasks. The difference in the task object’s type introduces a communication barrier between Parsl and RP. We overcame this challenge by implementing a mid-point component called “Task Translator”, with the following capabilities: (i) detect whether Parsl task is a pure Python function or a Python call to a Bash command; (ii) translate Parsl tasks into RP tasks; and (iii) update the status of Parsl tasks, according to callbacks from RP tasks.

Fig. 3 illustrates the translation of Parsl tasks into RP tasks. Each Parsl task is translated via a direct (1:1) mapping in accordance to the task submission criteria of Parsl’s DFK. Thus, tasks are created at application level and submitted to the executor one by one, iteratively.

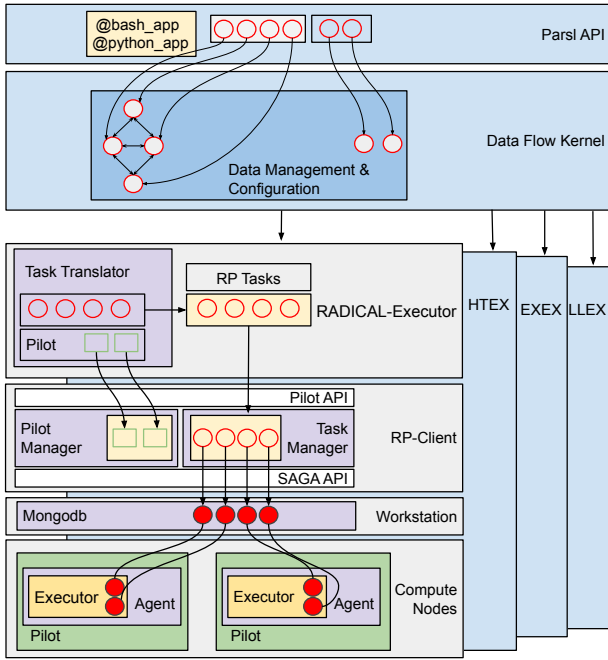


Fig. 3. RP-Parsl integration architecture.

#### D. Implementation

We use RP as an executor of Parsl and we call it the RADICAL-Executor. The RADICAL-Executor is shown in Fig. 3, the executor is a Python class that bootstraps RP when Parsl initializes it.

Once the DFK solves task dependencies, it initializes the RADICAL-Executor and passes the task object to it (Fig.3, RADICAL-Executor). Upon initialization, RADICAL-Executor pulls the number of CPU and GPU cores required by the tasks, the remote HPC platform on which to execute the tasks, and the amount of walltime for which to hold the resources. Then, the executor starts a new RP session and creates the Pilot Manager and the Task Manager. Immediately after the initialization process, Parsl DFK starts the executor, the latter constructs the pilot, and adds the pilot to the Pilot Manager.

Submitting and executing Parsl tasks using RP require translating those tasks into task objects that can be interpreted by RP. Each task object has a set of properties, including, for example, the executable’s name, its type, its arguments (if any), the number and type of resources, the number of processes and so on [29]. Once the DFK submits the Parsl task to the RADICAL-Executor, the Task translator unpacks, translates, and maps the Parsl task directly to the corresponding RP task object.

Simultaneously, Parsl DFK monitors the executor status and starts submitting Parsl tasks one by one to RP (Fig.3, RP-Client), once the executor components are ready. Eventually, RP submits the task to the Task Manager to be scheduled and executed (Fig.3, Compute Nodes). Depending on performance considerations, RP

can be configured to accumulate a certain amount of tasks and then bulk-submit them for execution. This would reduce latency when executing tasks on remote resources.

Note that Parsl does not require resource specification at task level, while RP requires to specify the number of cores and threads for both GPUs and CPUs for every task (or use default values). To enable the use of RP’s resource management capabilities in RP-Parsl, we extended Parsl’s API enabling users to define the number of CPU and GPU cores needed and the number of threads per task.

#### E. RP Executors

Message Passing Interface (MPI) is the most used message-passing model on HPC platforms. To support launching and executing of MPI Python functions, we implemented a RP single/multi-node MPI function executor shown in Fig. 4. The executor is built on the top of `mpi4py` [27] and `MPI-CommExecutor` to: (i) support a task-based master-worker paradigm; and (ii) support MPI-1 and MPI-2 implementations for shared and non-shared memory computers, respectively [30].

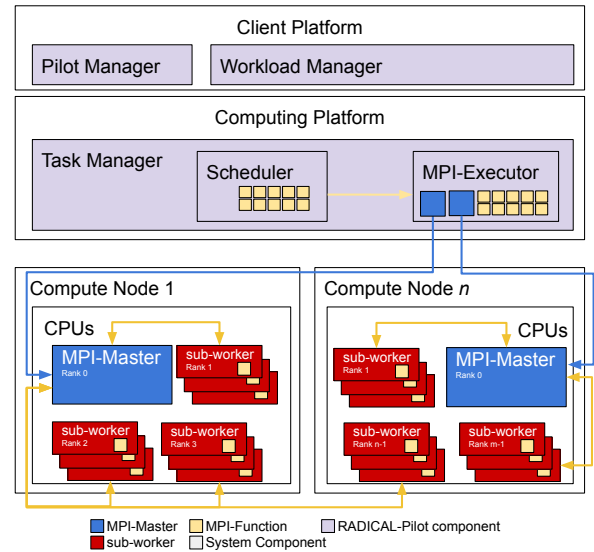


Fig. 4. RADICAL-Pilot multi-node MPI function executor.

Unlike other MPI function executors [31], [32], our MPI executor is designed to launch itself via a user-specified MPI launch method and scale to multiple nodes. Once the MPI function executor is launched, it spawns an MPI-Master, loads the `mpi4py` environment and starts the `mpi4py` `MPI-CommExecutor`. Eventually, the MPI-Master spawns several sub-workers via the `MPI-CommExecutor` that can concurrently work on single or multiple nodes. Every MPI-Master is responsible for executing a set of Python functions and performing MPI collective communications among the workers.

Our MPI function executor supports two communication patterns: MPI-Map and MPI-Pool. The MPI-Map pattern allows the function to be executed asynchronously,

with several concurrent calls made to the same function. It takes an iterable set of data that can be partitioned into small subsets. The MPI-Master collectively sends and gathers those data partitions to and from the sub-workers. The MPI-Pool pattern instead executes an MPI function with a master-worker approach, using a pool of processes specified for every function. Similar to the MPI-Map pattern, the results are collected by the MPI-Master from every sub-worker.

To ship the functions from the client-side to the Agent-side and execute them via the RP MPI/non-MPI executor, we implemented a `dill` based [33] function serialization utility that offers: (i) a fast and lightweight function serialization/deserialization from a file or a binary object; (ii) the ability to save the state of the Python interpreter to preserve the function dependencies; (iii) a fault-tolerance approach that switches between file and objects serialization/deserialization in case one of them failed.

## V. EXPERIMENTS AND EVALUATION

Table I shows the setup of our experiments. We use SDSC Comet to run Experiment 1 and 3, and SDSC Comet and TACC Frontera for Experiment 2. Comet has two types of nodes: “compute” nodes with 1 CPU with 24 cores, and “gpu” nodes with either 4 Nvidia Kepler K80 GPUs or 4 Nvidia Pascal P100 GPUs. On Frontera, every node has 1 CPU with 56 cores and no GPUs.

We use three metrics for the experiments: Total Processing Time (TPT); Throughput (TS); and Total Time to Execution (TTX). TPT is the time spent by the executor to finish executing all the tasks of a workload. TS is the number of tasks executed per second, calculated by dividing the total number of tasks by TPT. TTX is the total amount of time taken by the tasks to finish executing. Note that TPT measures the time the executor spent to make the resources busy, excluding any waiting or idle time. In contrast, TTX measures the time the workload spent to finish the execution of all tasks on those resources, including idle and waiting time.

Experiments 1 and 2 measure the TPT and TS of the stand alone function executor and of the MPI-function executor presented in §IV, as a function of the number of tasks. Experiment 3 characterizes the TTX and the integration overheads with the two use cases described in §III. Together, these experiments enable us to characterize the performance of the integrated system RP-Parsl (§IV) and of the Python function executors with different resources, task heterogeneity and scale on HPC resources.

### A. Experiment 1: Function Executor Scalability

We characterize the strong and weak scaling of the function executor in terms of TPT and TS on Comet. Fig. 5a shows the strong scaling of our function executor’s TPT and TS, using 49,000 no-op Python function tasks while doubling the number of nodes at each run. TPT is relatively consistent between 2, 4, 32 and 64 nodes, considering

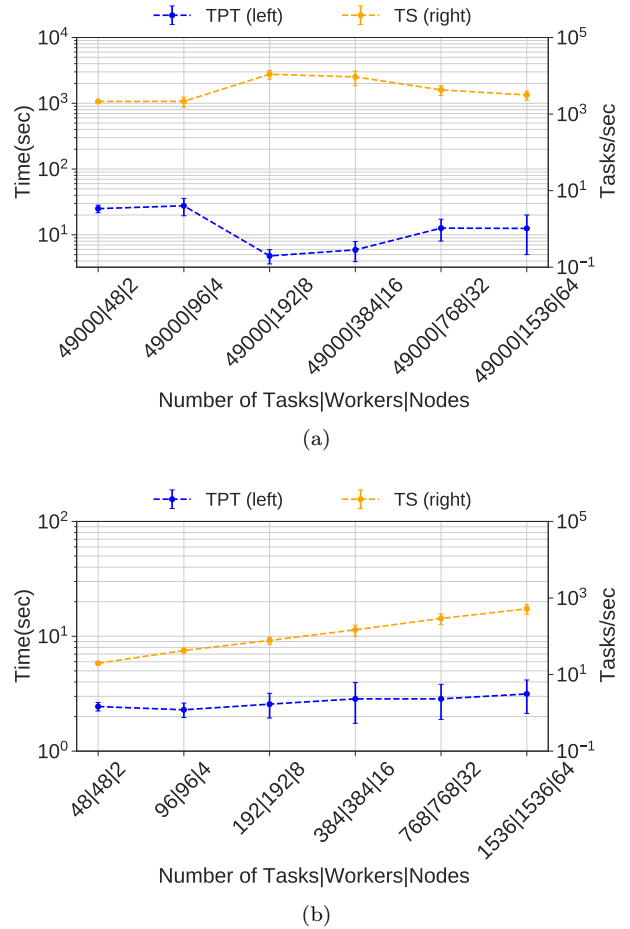


Fig. 5. Experiment 1: Function executor strong scaling (a) and weak scaling (b) while executing 49,000 and 48–1536 no-op Python function tasks respectively on Comet.

the error bars between 4, 32, and 64 nodes. Further, the TPT shows a linear decrease on 8 and 16 nodes.

We investigated the TPT’s behavior by looking at the distribution of the worker’s duration. Our analysis showed a bimodal distribution for the runs with 8 and 16 nodes with two peaks of 0.2s and 0.8s, consistent with the observed fluctuations of TPT. Unlike the runs with 8 and 16 nodes, we did not observe bimodality between 2, 4, 32, and 64. Further, most of the worker’s duration from 8 and 16 nodes show significantly shorter processing time with 2, 4, 32, and 64 nodes, which explains the performance gain of the TPT on these runs.

To understand the cause of the bimodal distribution, we measured the frequency performance of Comet CPU while running 1000 ‘no-op’ tasks sequentially. We noticed that the processor’s speed alternates between 1508 MHz and 2319 MHz, resulting in varying processing time for a single execution request. In conclusion, we owe the increasing and decreasing of TPT and TS to the processor speed alternation which affects the performance [34] of the executor as we observed in Fig. 5a.

TS in Fig. 5a reflects the inverse of the processing time analysis. The linear increase of TS between 4 and 8 nodes

TABLE I  
EXPERIMENTS 1–3: SETUP. WS/SS = WEAK AND STRONG SCALING; GEO = GEOLOCATION; IWP = ICE WEDGE POLYGONS.

ID	Experiment Type	Platform	Nodes	Task Type	CPUs(cores)	GPUs
1	Non-MPI executor WS/SS	Comet	$2^2 - 2^6$	Homogeneous	$\#nodes * 24$	N/A
2	MPI executor WS/SS	Comet	$2^2 - 2^6$	MPI-Homogeneous	$\#nodes * 24$	N/A
	MPI executor WS/SS	Frontera	$2^2 - 2^9$	MPI-Homogeneous	$\#nodes * 56$	N/A
3	Geo/IWP WS/SS	Comet	$2^1 - 2^3$	Heterogeneous	$\#nodes * 24$	$2^3 - 2^5$

and sublinear between 8 and 16 confirms our analysis of the TPT. The amount of tasks that workers can process is lower with runs from 2, 32, and 64 nodes.

Fig. 5b shows the weak scaling of our executor’s TPT and TS. We increased the number of tasks and nodes proportionally from 48/2 tasks/nodes to 1536/64 tasks/nodes to maintain full concurrency. While we double the number of tasks/nodes, the TPT scales linearly between 2 and 64 nodes. Further, the error bars remain small across all of the data points, indicating a consistent performance across the measured scale. TS shows a slight linear increase with a significant overlapping in the error bars. The scaling behavior in Fig. 5b shows a strong positive correlation between the number of workers and TS, confirming that larger TS can be achieved with more workers.

### B. Experiment 2: MPI-Function Executor Scalability

We characterize the performance of the MPI-function executor on Comet and Frontera, measuring its strong and weak scaling in terms of TPT and TS. As TPT measures the processing time of the MPI function executor, including the aggregated overheads of launching the MPI infrastructure, we separate TPT and overheads to analyze and compare their respective contributions.

We use an homogeneous workload of Python functions that performs `sleep(5)`. We configured the executor to execute each MPI function across two compute nodes using `mpirun` [35] as the launch method and `mpi4py` for each function. Consistently, every function requires 48 ranks on Comet (24 cores per node) and 112 ranks on Frontera (56 cores per node).

1) *SDSC Comet*: Fig. 6a shows the strong scaling of our MPI executor’s TPT (blue, left y axis) and TS (orange, right y axis). We increase the number of nodes by a factor of 2 and fix the number of tasks to 32. TPT decreases linearly from 202.5s on 4 nodes to 24.54s on 32 nodes showing an efficient scaling behavior. TS shows a consistent linear increase with the number of nodes and it reaches a maximum value of 0.7 tasks/s on 64 nodes. The error bars remain small across all the data points, indicating consistent behavior across the experiment’s scale.

Fig. 6b shows the weak scaling behavior of the MPI executor. TPT (blue, left y axis) shows consistent scaling behavior between 4 and 16 nodes and increases sublinearly between 16 and 64 nodes, likely due to the overheads of managing resource partitioning. TS increases linearly with the number of nodes reaching a maximum value of 1.3

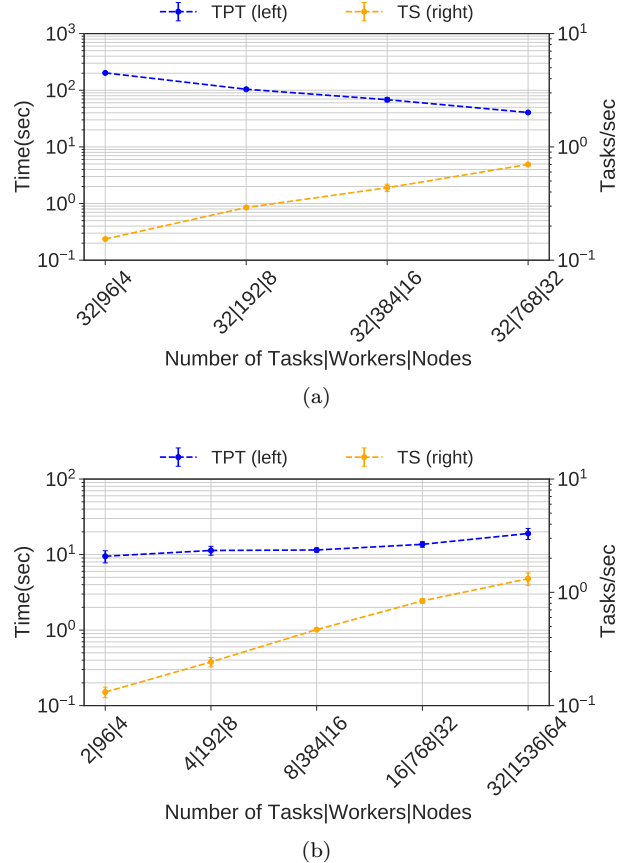
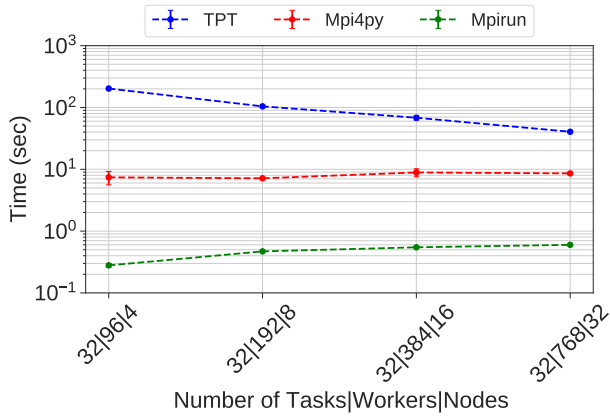


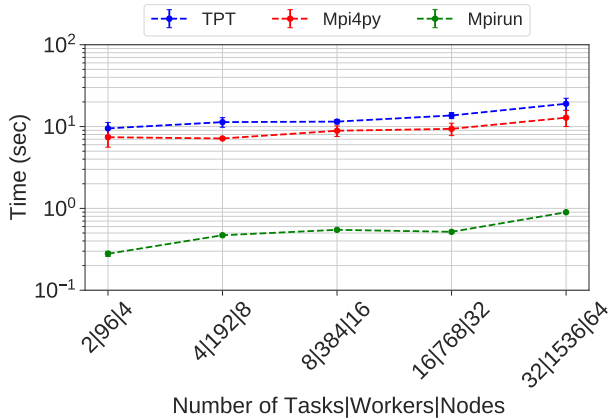
Fig. 6. Experiment 2: MPI Function executor strong scaling (a) and weak scaling (b) while executing 32 and 2–32 48 cores MPI Python function tasks on Comet.

task/s, while maintaining small error bars. The linear increase of TS in Figs. 6b and 6a shows a positive correlation between the number of workers and the number of tasks.

The MPI executor spends on average  $\sim 20$ s to execute a single 5s task so we further profiled the executions, isolating the dominant overheads. Fig. 7 shows two overheads of the executor’s TPT with strong (7a) and weak (7b) scaling runs: (i) `mpi4py` MPI-communicator initialization and low-level libraries calls (red); and (ii) `mpirun` startup time (green). `mpi4py` overhead is constant across both scaling, taking 10s on average to import the necessary libraries and setup a communicator of 48 ranks for each function task. As expected, `Mpirun` overhead increases with the number of resources, taking a maximum of 1s to launch 32 tasks over 64 nodes. The MPI function executor overhead is calculated as  $TPT - Mpi4py - Mpirun - TTX$  and accounts



(a)



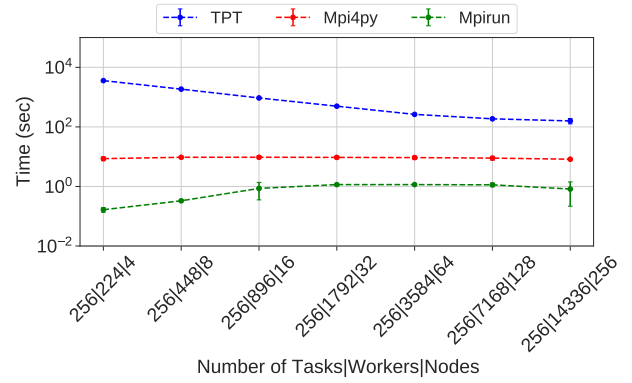
(b)

Fig. 7. Experiment 2: MPI Function executor TPT overheads for strong (a) and weak (b) scaling on Comet.

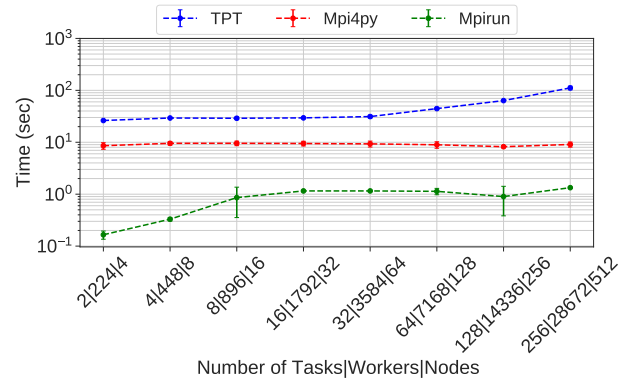
mostly for the time spent deserializing each MPI task. As such, it accumulates when deserializing tasks sequentially as when executing 32 2-nodes MPI tasks on 4 nodes.

Using a homogeneous workload allows us to study the baseline performance of the executor since it is more generalizable and easier to measure across different scales. Our MPI function executor requires that a new MPI communicator be constructed for every task, which, as shown by Figs. 7a and 7b, produces high overheads. Those overheads could be reduced by setting up the MPI communicator only once; however, the executor would be suitable only for homogeneous workloads in which each function requires the same number of ranks. For heterogeneous workloads composed of Python MPI functions with different requirements, the overheads seem unavoidable. Those overheads might be smaller with different MPI implementations, e.g., for functions not written in Python. Lowering task deserializing is also a priority to further reduce overheads with Python MPI functions.

2) *TACC Frontera*: We used the same experiment setting of Comet to characterize strong and weak scaling of the MPI function executor on Frontera at larger scale. Fig. 8a shows the strong scaling of the MPI executor’s



(a)



(b)

Fig. 8. Experiment 2: MPI Function executor strong scaling (a) and weak scaling (b) while executing 256 and 2–256 112 cores MPI Python function tasks on Frontera.

TPT (blue) alongside `mpi4py` overhead (red) and `mpirun` overhead (green). We use 256 tasks and increase the number of nodes by a factor of 2 at each run. The TPT decreases linearly between 4 and 64 nodes and sublinearly between 64 and 512 nodes, maintaining small error bars.

The executor shows a TPT of  $\sim 26$ s for a single 5s task and grows proportionally with the number of tasks. `mpi4py` in Fig. 8a maintains an overhead of  $\sim 11$ s per task across different nodes, while `mpirun` overhead is  $\sim 0.4$ s between 4 and 16 nodes and  $\sim 1.3$ s between 16 and 256 nodes. Finally, RP’s MPI executor took  $\sim 57\%$  of the TPT ( $\sim 14$ s) to execute single MPI task with 112 ranks across 2 nodes.

Fig. 8b shows the weak scaling of the executor in terms of TPT (blue). The TPT remains stable between 4 and 64 nodes and linearly increases between 64 and 512 nodes. Both `mpi4py` overhead (red) and `mpirun` overhead (green) are the same as measured with the strong scaling runs (Fig. 9a):  $\sim 11$ s and  $\sim 1$ s respectively.

Comparing the results from Comet’s in V-B1, Fig. 6a to the results in Fig. 8a, we conclude that, as expected, the cost of launching bigger MPI task with 112 ranks compared to 48 ranks grows with the scale, since `mpi4py` spends more time to construct larger MPI-communicator.

Fig. 9a shows the strong scaling of executor in terms of TS (orange). Consistent with TPT (blue), TS increases



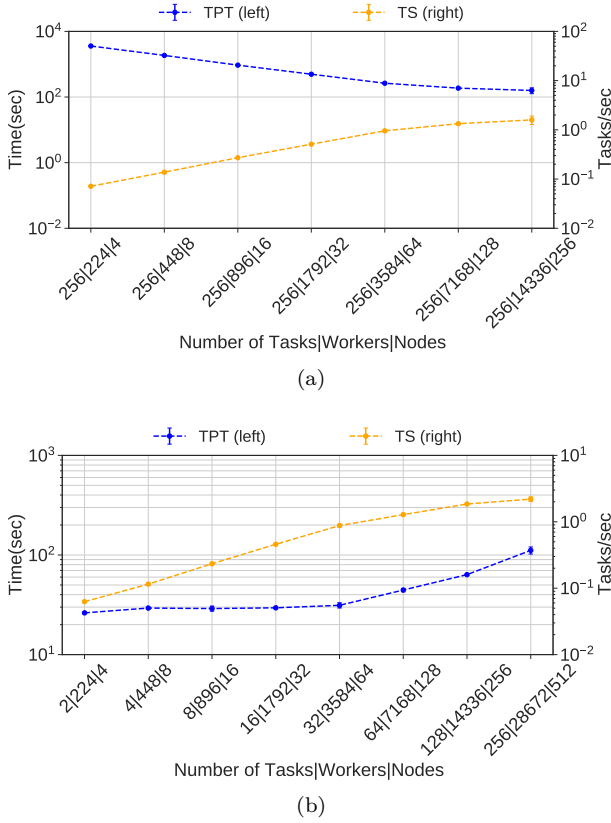


Fig. 9. Experiment 2: MPI Function executor TPT overheads for strong (a) and weak (b) scaling on Comet.

linearly between 4 and 64 nodes and sublinearly between 64 and 512 nodes. The strong scaling behavior between 4 and 64 nodes indicates that the executor consistently performs at its best with small error bars. In addition, the performance sublinearly decays between 64 and 256 nodes. The weak scaling of the executor’s TS (orange) in Fig. 9b shows a linear increase between 4 and 64 nodes and sub-linear increase between 64 and 512 nodes, and consistent behavior with TPT (blue).

We compare the scaling behavior of Frontera to Comet’s scaling in §V-B1, and we conclude that the MPI function executor’s TPT increases proportionally with the number of tasks, and the executor’s overheads grows bigger with the number of ranks per task. The MPI executor scales efficiently between 4 and 64 nodes on Frontera and 4 and 32 nodes on Comet, but given the proportional increase of the overheads between 64 and 512 nodes, performance starts to deteriorate at a larger scale. Initializing a new MPI communicator for every task is expensive but necessary in presence of heterogeneous functions. For short-running and homogeneous function tasks, a more performant design would set up the communicator only once. Thus, it is recommended to use the MPI function executor for long-running heterogeneous MPI functions to balance the overheads against the large execution time of each function.

TABLE II

EXPERIMENTS 3: RESULTS SUMMARY. WS/SS = WEAK AND STRONG SCALING; #N = NUMBER OF COMPUTE NODES; GEO = GEOLOCATION; IWP = ICE WEDGE POLYGONS; TTX = TOTAL TIME TO COMPLETION; OVH = INTEGRATION OVERHEAD

Exp. Type	#N	TTX	RP OVH	RP-Parsl OVH
GEO SS	2	2817.21 ± 235	27.44 ± 17	49.94 ± 17
	4	1646.75 ± 247	20.31 ± 7	57.16 ± 10
	8	1236.43 ± 392	27.54 ± 13	57.20 ± 12
GEO WS	2	132.50 ± 6	32.84 ± 12	64.47 ± 4
	4	186.28 ± 7	27 ± 5	57.65 ± 8
	8	278.33 ± 47	26.33 ± 2	57.60 ± 8
IWP SS	2	7011.76 ± 349	85.4 ± 1	136.44 ± 7
	4	5276.48 ± 1280	85 ± 3	139 ± 15
	8	2901.64 ± 563	88 ± 6	151.9 ± 37
IWP WS	2	861.76 ± 8	82.92 ± 4	124.26 ± 3
	4	899.37 ± 36	91.07 ± 1	137.54 ± 18
	8	896.56 ± 7	85.01 ± 3	138.50 ± 9

### C. Experiment 3: Use Cases Scalability

We use RP-Parsl to implement and execute two use cases that are required to run at scale. We characterize the strong and weak scaling of the Geolocation and the IWP use cases (§III) on Comet.

The Geolocation use case requires a workflow with concurrent heterogeneous Python functions, and the IWP use case requires a workload of heterogeneous MPI-functions that runs concurrently on multiple nodes. Thus, those use cases offer the opportunity to characterize the behavior of both RP-Parsl and our MPI function executor with production tasks on a production HPC platform.

We characterize the strong and the weak scaling of RP-Parsl integration overheads (OVH) and total time to completion (TTX), and we summarize our experiment results in Table II. We measure the integration overheads as the combination of Parsl and RP overheads. Parsl’s overhead includes the amount of time taken by Parsl to: (1) start the executor; (2) build the DAG of the tasks; (3) solve the data dependencies among all tasks; (4) submit the tasks to the executor; and (5) shutdown and cleanup both the executor and the integration components. RP’s overhead consists of the amount of time taken by RADICAL-Pilot to start the runtime system and manage the tasks’ execution, including the overheads of the (non)-MPI executors.

1) *Geolocation*: The Geolocation workflow consists of the two heterogeneous tasks described in §III. The workflow concurrently launches two GPU tasks on a single GPU, and the number of concurrent geolocation workflows is bounded by the number of GPUs available. Consequently, we configured RP-Parsl to submit and execute two GPU tasks for every GPU, with a maximum of 64 concurrent workflows on 8 nodes.

Figs. 10a and 10b show the strong and weak scaling of RP-Parsl in terms of TTX (red), RP overheads (purple) and RP-Parsl overheads (blue). TTX shows sublinear strong and weak scaling but, importantly, RP-Parsl and RP overheads are constant across all runs. This shows

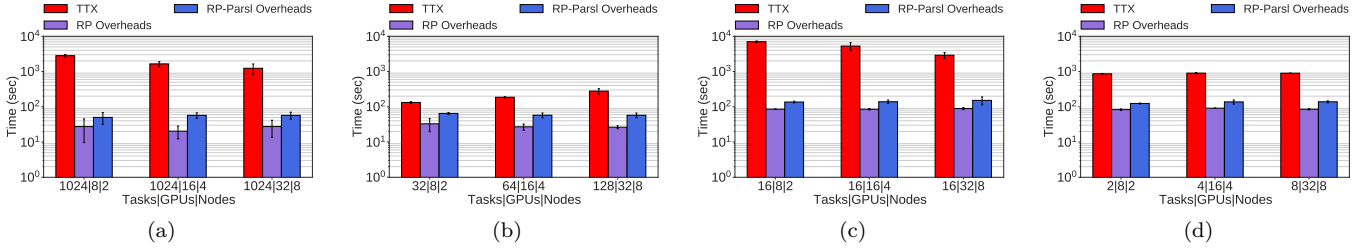


Fig. 10. Experiment 3: Strong and weak scaling of the Geolocation and Ice Wedge Polygons (IWP) use cases presented in §III. RP-Parsl overheads include RP overheads and represent the total overhead of the execution. RP overheads represent the time spent by RP and its executor to manage the execution of the workflow Python functions.

that the overheads are invariant of the number of tasks concurrently and sequentially executed by RP-Parsl. Further, as RP-Parsl overheads include also RP overheads, the cost of RP-Parsl is minimal compared to the TTX of the production workflows. RP overheads average at  $\sim 30$ s (see Table II), a value that becomes less relevant with scale and the consequent increase of TTX. As seen in §V-A, our function executor contributes 2s and 10s to RP overhead, confirming its suitability for production use cases.

2) *Ice Wedge Polygons (IWP)*: The IWP use case described in §III is implemented by using the Single Program Multiple Data (SPMD) MPI pattern, where tasks are split up and concurrently run on multiple cores with different inputs [36]. We configure RP-Parsl to use RP’s MPI function executor and execute the IWP workload with a SPMD pattern. We use 4 GPUs and 24 CPU cores per task, with a maximum of 8 concurrent tasks on Comet.

Figs. 10c and 10d show the strong and weak scaling of RP-Parsl with the IWP use case’s workflow. As with the Geolocation use case, overheads are invariant of the number of resources and tasks. That confirms that the performance of RP-Parsl is independent from the performance of the function tasks (TTX). RP overhead is  $\sim 86$ s, almost three times larger than that measured with the Geolocation use case. That is consistent with the MPI executor’s performance characterized in §V-B. Overall, RP-Parsl overheads are still marginal compared to the TTX of the use case but the magnitude of the executor overheads suggests that it is best suited to support use cases with longer TTX and/or larger MPI tasks.

## VI. CONCLUSIONS AND FUTURE WORK

In this paper, we described the integration of RADICAL-Pilot’s pilot capabilities with Parsl’s workflow management capabilities to enable the execution of production workflows on diverse HPC platforms. The paper presents four main contributions: (1) a case study about the engineering process of integrating two middleware systems, independently developed by diverse research groups; (2) an analysis of the design of an executor for (non)-MPI Python functions tailored to HPC resources; (3) a performance characterization of both the integrated systems and the proposed executor on two HPC platforms, SDSC Comet and TACC Frontera; and (4) the

use of the integrated system and the executor to execute production workflows for real use cases.

The RP-Parsl integration shows that integrating independent middleware systems requires an analysis of their capabilities, execution and state models, private and public APIs, and performance bottlenecks. We showed that, based on that analysis, the integration’s engineering effort can be reduced, while avoiding expensive rewriting of the existing code bases. Nonetheless, extensions to user-facing APIs might not be avoidable, based on assumptions made across the stack of information availability.

Experiments showed that the overheads of RP-Parsl are invariant across number and type of resources, and number of function tasks executed. This confirmed that our integration approach, based on weakly-coupling the two system via a light-weight, stand-alone interface, does not introduce major overheads when executing heterogeneous workflows on HPC resources. Nonetheless, experiments also showed that further optimization is needed when executing MPI Python functions at scale. Our experiments show that Python object serialization and `mpi4py` are the clear targets of such optimizations.

Important also to note the distinction between performance of workloads with homogeneous and heterogeneous MPI function tasks. The analysis of our MPI Python function executor and its performance characterization shows that for homogeneous workloads, overheads can be drastically reduced by launching the MPI infrastructure only once. This identifies a new space of optimization into RP scheduler with the use of classification algorithms for partitioning tasks into homogeneous subsets. Such subsets could be scheduled into dedicated masters that, in turn, could setup only once their own MPI infrastructure.

The contributions of this paper also confirm that using integration between independent middleware components is a viable approach to reduce capability duplication across middleware. This is particularly important when considering the challenges posed by the upcoming exascale HPC platforms. Without an ecosystem populated by specialized, efficient, effective and well-maintained software systems that can be integrated to offer end-to-end capabilities to their user communities, it will be difficult to fully realize the potential of exascale resources to execute workflows and promote discovery.

## REFERENCES

- [1] M. Turilli, Y. N. Babuji, A. Merzky, M. T. Ha, M. Wilde, D. S. Katz, and S. Jha, "Analysis of distributed execution of workloads," *arXiv preprint arXiv:1605.09513*, 2016.
- [2] A. Luckow, I. Paraskevagos, G. Chantzialexiou, and S. Jha, "Hadoop on hpc: Integrating hadoop and pilot-based dynamic resource management," in *2016 IEEE International Parallel and Distributed Processing Symposium Workshops (IPDPSW)*, 2016, pp. 1607–1616.
- [3] M. Turilli, V. Balasubramanian, A. Merzky, I. Paraskevagos, and S. Jha, "Middleware building blocks for workflow systems," *Computing in Science & Engineering*, vol. 21, no. 4, pp. 62–75, 2019.
- [4] A. Merzky, M. Turilli, M. Maldonado, M. Santcroos, and S. Jha, "Using pilot systems to execute many task workloads on supercomputers," 2018.
- [5] A. Merzky, M. Turilli, M. Titov, A. Al-Saadi, and S. Jha, "Design and performance characterization of radical-pilot on leadership-class platforms," *TDPS, Special Section on Innovative R&D toward the Exascale Era*, 2021.
- [6] Y. Babuji, A. Woodard, Z. Li, D. S. Katz, B. Clifford, R. Kumar, L. Lacinski, R. Chard, J. M. Wozniak, I. Foster, M. Wilde, and K. Chard, "Parsl: Pervasive parallel programming in python," in *Proceedings of the 28th International Symposium on High-Performance Parallel and Distributed Computing*, ser. HPDC '19. New York, NY, USA: Association for Computing Machinery, 2019, p. 25–36. [Online]. Available: <https://doi.org/10.1145/3307681.3325400>
- [7] I. Altintas, C. Berkley, E. Jaeger, M. Jones, B. Ludascher, and S. Mock, "Kepler: an extensible system for design and execution of scientific workflows," in *Proceedings. 16th International Conference on Scientific and Statistical Database Management, 2004.*, 2004, pp. 423–424.
- [8] K. Shvachko, H. Kuang, S. Radia, and R. Chansler, "The hadoop distributed file system," in *2010 IEEE 26th Symposium on Mass Storage Systems and Technologies (MSST)*, 2010, pp. 1–10.
- [9] J. Wang, D. Crawl, and I. Altintas, "Kepler + hadoop: A general architecture facilitating data-intensive applications in scientific workflow systems," in *Proceedings of the 4th Workshop on Workflows in Support of Large-Scale Science*, ser. WORKS '09. New York, NY, USA: Association for Computing Machinery, 2009. [Online]. Available: <https://doi.org/10.1145/1645164.1645176>
- [10] M. Wilde, M. Hategan, J. M. Wozniak, B. Clifford, D. S. Katz, and I. Foster, "Swift: A language for distributed parallel scripting," *Parallel Computing*, vol. 37, no. 9, pp. 633–652, 2011, emerging Programming Paradigms for Large-Scale Scientific Computing. [Online]. Available: <https://www.sciencedirect.com/science/article/pii/S0167819111000524>
- [11] Shaffer, Li, Tovar, Babuji, Dasso, Surma, Chard, Foster, and Thain, "Lightweight function monitors for fine-grained management in large scale python applications," in *International Parallel and Distributed Processing Symposium (IPDPS)*, 2021.
- [12] P. Bui, D. Rajan, B. Abdul-Wahid, J. Izaguirre, and D. Thain, "Work queue + python: A framework for scalable scientific ensemble applications," in *Workshop on python for high performance and scientific computing at sc11*. Citeseer, 2011.
- [13] J. L. Peterson, R. Anirudh, K. Athey, B. Bay, P.-T. Bremer, V. Castillo, F. D. Natale, D. Fox, J. A. Gaffney, D. Hysom, S. A. Jacobs, B. Kailkhura, J. Koning, B. Kustowski, S. Langer, P. Robinson, J. Semler, B. Spears, J. Thiagarajan, B. V. Essen, and J.-S. Yeom, "Merlin: Enabling machine learning-ready hpc ensembles," 2019.
- [14] F. D. Natale, "Maestro workflow conductor," <https://github.com/LLNL/maestrowf>, 2019.
- [15] D. H. Ahn, J. Garlick, M. Grondona, D. Lipari, B. Springmeyer, and M. Schulz, "Flux: A next-generation resource management framework for large hpc centers," in *2014 43rd International Conference on Parallel Processing Workshops*, 2014, pp. 9–17.
- [16] T. Öhberg, A. Ernstsson, and C. Kessler, "Hybrid cpu-gpu execution support in the skeleton programming framework skepu," *The Journal of Supercomputing*, vol. 76, no. 7, pp. 5038–5056, 2020.
- [17] C. Augonnet, S. Thibault, R. Namyst, and P.-A. Wacrenier, "Starpu: A unified platform for task scheduling on heterogeneous multicore architectures," in *Euro-Par 2009 Parallel Processing*, H. Sips, D. Epema, and H.-X. Lin, Eds. Berlin, Heidelberg: Springer Berlin Heidelberg, 2009, pp. 863–874.
- [18] J. Enmyren and C. W. Kessler, "Skepu: A multi-backend skeleton programming library for multi-gpu systems," in *Proceedings of the Fourth International Workshop on High-Level Parallel Programming and Applications*, ser. HLPP '10. New York, NY, USA: Association for Computing Machinery, 2010, p. 5–14. [Online]. Available: <https://doi.org/10.1145/1863482.1863487>
- [19] D. G. Lowe, "Distinctive image features from scale-invariant keypoints," *Int. J. Comput. Vision*, vol. 60, no. 2, p. 91–110, Nov. 2004. [Online]. Available: <https://doi.org/10.1023/B:VISI.0000029664.99615.94>
- [20] M. A. Fischler and R. C. Bolles, "Random sample consensus: A paradigm for model fitting with applications to image analysis and automated cartography," *Commun. ACM*, vol. 24, no. 6, p. 381–395, Jun. 1981. [Online]. Available: <https://doi.org/10.1145/358669.358692>
- [21] A. Al-Saadi, "Scalable algorithm and workload execution for geo locating satellite imagery," Master's thesis, Rutgers The state university of New Jersey, 2020.
- [22] G. Bradski, "The OpenCV Library," *Dr. Dobbs's Journal of Software Tools*, 2000.
- [23] I. H. Mtir, K. Kaaniche, P. Vasseur, and M. Chtourou, "False positive outliers rejection for improving image registration accuracy - application to road traffic aerial sequences," in *ICINCO*, 2012.
- [24] C. Witharana, M. A. E. Bhuiyan, A. K. Liljedahl, M. Kanevskiy, T. Jorgenson, B. M. Jones, R. Daanen, H. E. Epstein, C. G. Griffin, K. Kent, and M. K. Ward Jones, "An object-based approach for mapping tundra ice-wedge polygon troughs from very high spatial resolution optical satellite imagery," *Remote Sensing*, vol. 13, no. 4, 2021. [Online]. Available: <https://www.mdpi.com/2072-4292/13/4/558>
- [25] M. Turilli, M. Santcroos, and S. Jha, "A comprehensive perspective on pilot-job systems," *ACM Comput. Surv.*, vol. 51, no. 2, Apr. 2018. [Online]. Available: <https://doi.org/10.1145/3177851>
- [26] P. . Documentation, "Concurrent.futures - launching parallel tasks," 2020.
- [27] L. Dalcín, R. Paz, and M. Storti, "Mpi for python," *Journal of Parallel and Distributed Computing*, vol. 65, no. 9, pp. 1108–1115, 2005. [Online]. Available: <https://www.sciencedirect.com/science/article/pii/S0743731505000560>
- [28] M. Turilli, F. Liu, Z. Zhang, A. Merzky, M. Wilde, J. Weissman, D. S. Katz, and S. Jha, "Integrating abstractions to enhance the execution of distributed applications," in *2016 IEEE International Parallel and Distributed Processing Symposium (IPDPS)*. IEEE, 2016, pp. 953–962.
- [29] R. development team, "RADICAL-Pilot application programming interface (API)," 2021, [Accessed 19-May-2021]. [Online]. Available: [\url{https://radicalpilot.readthedocs.io/en/stable/apidoc.html}](https://radicalpilot.readthedocs.io/en/stable/apidoc.html)
- [30] "Mpi: A message passing interface," in *Supercomputing '93: Proceedings of the 1993 ACM/IEEE Conference on Supercomputing*, 1993, pp. 878–883.
- [31] P. Hadjidoukas, A. Bartezzaghi, F. Scheidegger, R. Istrate, C. Bekas, and A. Malossi, "torcpy: Supporting task parallelism in python," *SoftwareX*, vol. 12, p. 100517, 2020. [Online]. Available: <https://www.sciencedirect.com/science/article/pii/S2352711020300091>
- [32] S. Hudson, J. Larson, S. M. Wild, D. Bindel, and J.-L. Navarro, "libEnsemble users manual," Argonne National Laboratory, Tech. Rep. Revision 0.7.1, 2020. [Online]. Available: <https://buildmedia.readthedocs.org/media/pdf/libensemble/latest/libensemble.pdf>
- [33] M. McKerns, L. Strand, T. Sullivan, A. Fang, and M. Aivazis, "Building a framework for predictive science," *Proceedings of the 10th Python in Science Conference*, 02 2012.

- [34] P. Koutsovasilis, C. Antonopoulos, N. Bellas, S. Lalis, G. Papadimitriou, A. Chatzidimitriou, and D. Gizopoulos, "The impact of cpu voltage margins on power-constrained execution," *IEEE Transactions on Sustainable Computing*, vol. PP, pp. 1–1, 12 2020.
- [35] "mpirun," <https://linux.die.net/man/1/mpirun>, 2021, accessed: 2021-04-21.
- [36] F. Darema, *SPMD Computational Model*. Boston, MA: Springer US, 2011, pp. 1933–1943. [Online]. Available: [https://doi.org/10.1007/978-0-387-09766-4\\_26](https://doi.org/10.1007/978-0-387-09766-4_26)